Catalysis Today xxx (2016) xxx–xxx

Contents lists available at ScienceDirect

Catalysis Today

journal homepage: www.elsevier.com/locate/cattod

The effect of oxidative and reductive treatments of titania-supported metal catalysts on the pairwise hydrogen addition to unsaturated hydrocarbons

Oleg G. Salnikov[a,b,*], Dudari B. Burueva[a,b], Evgeniy Yu. Gerasimov[c,b], Andrey V. Bukhtiyarov[c,b], Alexander K. Khudorozhkov[c,b], Igor P. Prosvirin[b,c], Larisa M. Kovtunova[c,b], Danila A. Barskiy[a,d], Valerii I. Bukhtiyarov[c,b], Kirill V. Kovtunov[a,b], Igor V. Koptyug[a,b,*]

[a] Laboratory of Magnetic Resonance Microimaging, International Tomography Center, SB RAS, 3A Institutskaya St., 630090 Novosibirsk, Russia
[b] Novosibirsk State University, 2 Pirogova St., 630090 Novosibirsk, Russia
[c] Laboratory of Surface Science, Boreskov Institute of Catalysis, SB RAS, 5 Acad. Lavrentiev Pr., 630090 Novosibirsk, Russia
[d] Department of Radiology and Radiological Sciences, Institute of Imaging Science, Vanderbilt University, 1161 21st Avenue South, Medical Center North, AA-1105, Nashville, TN 37232-2310, USA

ARTICLE INFO

Article history:
Received 5 October 2015
Accepted 5 February 2016
Available online xxx

Keywords:
Parahydrogen-induced polarization (PHIP)
Hydrogenation
Heterogeneous catalysis
X-ray photoelectron spectroscopy (XPS)
Transmission electron microscopy (TEM)

ABSTRACT

Heterogeneous hydrogenation of unsaturated compounds with parahydrogen is a highly promising technique for boosting the sensitivity of magnetic resonance spectroscopy and imaging by hyperpolarizing reaction products in gaseous and liquid phases, and potentially reaction intermediates as well. This demands an efficient heterogeneous catalyst providing both the high selectivity toward pairwise hydrogen addition (i.e., ability to incorporate both H atoms of H_2 molecule in the same product molecule) as well as sufficient overall hydrogenation activity. In this work, we studied the influence of oxidative and reductive treatments of the supported metal catalysts on the NMR signal enhancements provided by parahydrogen-induced polarization (PHIP) effects in hydrogenation of propene, propyne, 1,3-butadiene and 1-butyne. The 5 wt% titania-supported Pt, Pd, Rh and Ir catalysts used here were characterized by X-ray photoelectron spectroscopy (XPS) and high-resolution transmission electron microscopy (HRTEM). Generally, the preliminarily reduced catalysts were found to be more efficient than the oxidized ones. For instance, while the reduced Ir/TiO_2 catalyst provided the intense PHIP NMR signals, its oxidized counterpart showed almost no activity in hydrogenation. For the oxidized Pd/TiO_2 catalyst, HRTEM revealed the formation of titania pedestals under large (ca. 5–7 nm) PdO nanoparticles. At the same time, the small (ca. 1 nm) partially reduced $Pd^{\delta+}$ particles were observed on the facets of TiO_2 support. These changes in catalyst structure led to a significant decrease in pairwise hydrogen addition selectivity.

1. Introduction

Nowadays, methods based on nuclear magnetic resonance (NMR), such as magnetic resonance spectroscopy (MRS) and magnetic resonance imaging (MRI), are unique analytical tools which are widely and routinely used in chemistry, medicine, and many other areas of research and practice. In the context of *operando* studies in catalysis [1–5], the MRI/MRS toolkit can be useful for conducting mechanistic studies of catalytic processes and for characterizing the behavior of operating model catalytic reactors. In particular, this toolkit allows one to map in situ the distribution of the liquid phase within the catalyst bed, to directly visualize various dynamic processes, and to evaluate local reactant-to-product conversion [6–8]. However, the NMR-based techniques have a significant drawback of low intrinsic sensitivity. One of the efficient ways to overcome this problem is the use of nuclear spin hyperpolarization techniques [9,10], e.g., dynamic nuclear polarization (DNP) [11] for hyperpolarization of solids, liquids or solutions, spin-exchange optical pumping (SEOP) [12] for hyperpolarization of gases, and parahydrogen-induced polarization (PHIP) [13,14] which can be successfully utilized for hyperpolarization of both

* Corresponding authors at: International Tomography Center, SB RAS, 3A Institutskaya St., 630090 Novosibirsk, Russia.
E-mail addresses: koptyug@tomo.nsc.ru, salnikov@tomo.nsc.ru (I.V. Koptyug).

http://dx.doi.org/10.1016/j.cattod.2016.02.030
0920-5861/

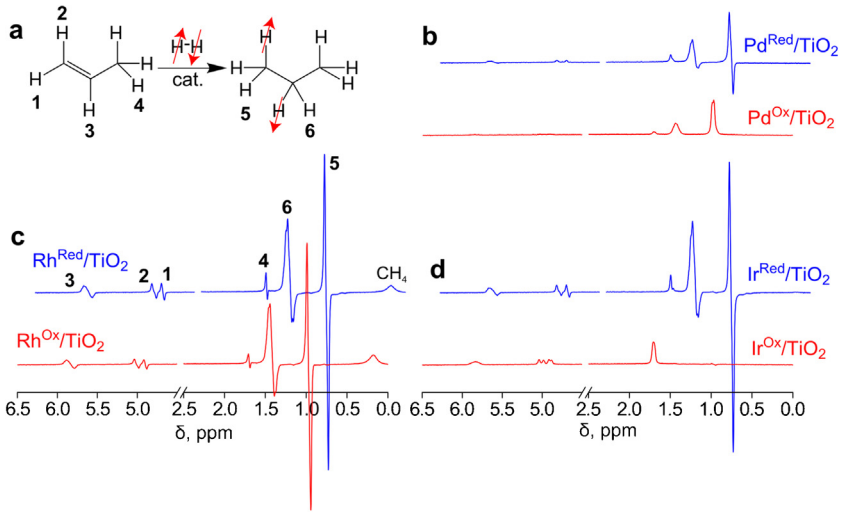

Fig. 1. (a) The reaction scheme of propene hydrogenation; (b–d) ^{1}H NMR spectra acquired during propene hydrogenation with p-H_2 at 100 °C over Pd^{Red}/TiO_2 and Pd^{Ox}/TiO_2 catalysts (b), over Rh^{Red}/TiO_2 and Rh^{Ox}/TiO_2 catalysts (c); and over Ir^{Red}/TiO_2 and Ir^{Ox}/TiO_2 catalysts (d). All spectra were acquired while the gas was flowing (4.1 mL/s) with 8 signal accumulations and are presented on the same vertical scale.

liquids and gases. The basis of PHIP is the exploitation of the singlet nuclear spin order of a parahydrogen molecule (p-H_2). However, because p-H_2 molecule has zero nuclear spin and therefore is NMR silent, the equivalence of the two H atoms of a p-H_2 molecule needs to be broken in order to get an enhanced NMR signal. This can be achieved via incorporation of p-H_2 in a product of a hydrogenation reaction [15]. Two major requirements for such hydrogenation reaction should be pointed out: (i) the reaction should proceed in a pairwise manner of hydrogen addition, meaning that two H atoms from the same p-H_2 molecule should be added to the same unsaturated substrate molecule; and (ii) the two nascent protons of p-H_2 molecule should end up in magnetically non-equivalent positions in the product molecule [16]. If both these requirements are met, the corresponding ^{1}H NMR signals of reaction products or intermediates can be significantly enhanced (up to 4–5 orders of magnitude in the case of standard NMR instruments) [16]. Moreover, the NMR lines get a characteristic line shape which makes it easy to detect PHIP phenomena and therefore the existence of pairwise hydrogen addition route [17].

Originally, PHIP effects were observed for the first time in homogeneous hydrogenations catalyzed by transition metal complexes, e.g. Wilkinson's catalyst [$Rh(PPh_3)_3Cl$] [13,18], due to a well-defined nature of an isolated catalytic center responsible for pairwise hydrogen addition. Later on, the PHIP technique was extensively utilized for mechanistic and kinetic studies of homogeneous hydrogenations catalyzed by transition metal complexes and clusters [17,19]. However, utilization of homogeneous PHIP to produce hyperpolarized fluids suitable for biomedical MRI studies is significantly complicated because of the presence of a toxic homogeneous catalyst in the reaction mixture, which cannot be easily removed from the solution after the reaction [20]. At first sight, this problem can be solved by the use of heterogeneous hydrogenation. However, the conventional catalysts for heterogeneous hydrogenation reaction are noble metal nanoparticles supported on porous oxides or carbon. For this type of catalysts, it is generally assumed that H_2 molecules adsorb dissociatively on the metal surface according to the established Horiuti-Polanyi mechanism [21]. Therefore, the complete randomization of H atoms involved in hydrogenation over the catalyst surface is expected, which should lead to a complete loss of spin correlation between the parahydrogen-derived protons and, consequently, to the absence of any PHIP effects in the NMR spectra of the products. Nevertheless, PHIP effects were observed in heterogeneous hydrogenation of unsaturated hydrocarbons over supported metal nanoparticles, meaning that the pairwise addition of hydrogen is possible with such catalysts [22]. Subsequent studies showed that PHIP effects can be observed in heterogeneous gas phase hydrogenations of various hydrocarbons such as propene [23,24], propyne [25], 1,3-butadiene and 1-butyne [26] as well as α,β-unsaturated carbonyl compounds [27] over several Pt, Pd, Rh and Ir [28] catalysts supported on Al_2O_3, SiO_2 and TiO_2 as well as over bulk metals and bulk metal oxides [29] (Pt, Rh, CaO, Cr_2O_3, CeO_2 [30], PtO_2, PdO and Rh_2O_3). Moreover, polarization was also successfully observed in liquid phase heterogeneous hydrogenations over supported metal nanoparticles [31–33]. Generally, the highest intensities of PHIP NMR signals were obtained in heterogeneous hydrogenations catalyzed by catalysts supported on TiO_2 [26]. The attempts to explain this fact led to an investigation of the influence of strong metal-support interaction (SMSI) effect on the pairwise hydrogen addition and PHIP [34]. However, in spite of all these studies the nature of active sites of supported metal catalysts which, contrary to the dissociative Horiuti-Polanyi mechanism, can add molecular hydrogen to the unsaturated substrates in a pairwise manner is still unclear [26]. Despite the fact that the contribution of pairwise hydrogen addition route is often not very high (ca. 1–3%) [26], finding an answer to this question is surely of great interest for chemical science as well as for possible practical applications. For instance, the production of hyperpolarized propane gas, which can be used as an efficient contrast agent for MRI of lungs, by heterogeneous hydrogenation of propene with p-H_2 was recently demonstrated with the use of titania-supported rhodium catalysts [23,35]. And without doubt, the fundamental understanding of the mechanism of pairwise hydrogen addition and the nature of active sites of supported metal catalysts responsible for pairwise hydrogen addition can help to design an efficient catalytic system with the largest contribution of the pairwise addition route to provide the maximum NMR signal enhancement suitable for comprehensive MRI studies.

It was mentioned above that TiO_2-supported metal catalysts exhibit higher contribution of pairwise hydrogen addition route and higher levels of PHIP NMR effects intensities compared to the metal catalysts on other supports. Therefore, the goal of this paper is to get some insight into the heterogeneous pairwise hydrogen addition phenomenon over titania-supported catalysts. The influence of metal oxidation state on the intensities of PHIP effects was investigated. For this purpose, a series of preliminary oxidized or reduced titania-supported Pt, Pd, Rh and Ir catalysts were prepared,

Please cite this article in press as: O.G. Salnikov, et al., The effect of oxidative and reductive treatments of titania-supported metal catalysts on the pairwise hydrogen addition to unsaturated hydrocarbons, Catal. Today (2016), http://dx.doi.org/10.1016/j.cattod.2016.02.030

characterized by XPS and HRTEM and tested in gas phase hydrogenation of propene, propyne, 1,3-butadiene and 1-butyne with p-H_2. The obtained results allowed us to make a conclusion that a fully reduced metallic state is generally more efficient in terms of pairwise hydrogen addition selectivity than the oxidized state.

2. Experimental

2.1. Catalysts preparation

The Pt/TiO_2, Pd/TiO_2, Rh/TiO_2 and Ir/TiO_2 catalysts (with 5 wt% metal loadings) were prepared using wet impregnation method. The TiO_2 powder (Hombifine N, S_{BET} = 107 m^2/g) was calcined at 500 °C for 2 h prior to use. In the case of the supported Pt, Pd and Rh catalysts, the aqueous solutions of corresponding Pt(II), Pd(II) and Rh(III) nitrates were used for impregnation. The preparation of nitrates solution is described in detail elsewhere [27]. In the case of the Ir/TiO_2 catalyst, the support was impregnated with aqueous $H_3[IrCl_6]$ solution which was prepared by dissolution of the commercial $IrCl_3$ (Sigma-Aldrich) in concentrated hydrochloric acid with subsequent evaporation to dryness and dissolution in water. The impregnation of TiO_2 support with corresponding precursor solutions was carried out for 1 h at room temperature. Then the solvent excess was evaporated and the obtained raw materials were dried in air at 120 °C for 4 h. The obtained M/TiO_2 samples were either calcined at 400 °C in air for 3 h (later denoted as M^{Ox}/TiO_2) or reduced in H_2 flow at 330 °C for 3 h (later denoted as M^{Red}/TiO_2) (M = Pt, Pd, Rh, Ir). Therefore, a total of eight different supported catalyst samples were prepared.

2.2. XPS experiments

The catalysts were characterized using X-ray photoelectron spectroscopy (XPS) before and after the hydrogenation of propene, propyne, 1,3-butadiene and 1-butyne. XPS spectra were recorded using SPECS spectrometer with PHOIBOS-150-MCD-9 hemispherical energy analyzer (Al Kα, irradiation, hν = 1486.6 eV, 200 W). The samples were supported onto the double-sided conducting copper scotch tape. Binding energy (BE) scale was preliminarily calibrated by the positions of the peaks of Au $4f_{7/2}$ (BE = 84.0 eV) and Cu $2p_{3/2}$ (BE = 932.67 eV) core levels. The binding energy of peaks was calibrated by the position of the Ti 2p peak (BE = 458.8 eV) corresponding to the titanium oxide as support. Pt, Pd and Rh foil, PtO, PdO, Rh_2O_3, Ir black and IrO_2 powders were used as reference samples. Pt 4f, Pd 3d, Rh 3d and Ir 4f regions peak fittings were performed using XPSPeak 4.1 software [36].

2.3. HRTEM experiments

The catalysts samples were studied by high-resolution transmission electron microcopy (HRTEM) method using JEM 2010 (JEOL, Japan) instrument with the accelerating voltage of 200 kV. Images were recorded using Soft Imaging System (Germany) CCD. The instrument was equipped with the energy-dispersive X-ray (EDX) spectrometer Phoenix (EDAX, USA) with the semiconductor Si(Li) detector with an energy resolution of 130 eV. The samples were dispersed in ethanol using an ultrasonic disperser UZD-1UCh2 and deposited on copper or molybdenum grids coated with a carbon hole film.

2.4. Catalytic hydrogenation experiments

Commercially available hydrogen, propene, 1,3-butadiene, propyne (Sigma-Aldrich, 98%) and 1-butyne (Sigma-Aldrich, ≥99%) were used as received. For PHIP experiments, hydrogen gas was enriched with parahydrogen from 25% (p-H_2 content in normal H_2) up to 83% using Bruker parahydrogen generator BPHG 90. The hydrocarbon/H_2 mixtures with 1:10 (in case of propyne) or 1:4 (in case of propene, 1,3-butadiene and 1-butyne) ratio were prepared in a gas cylinder.

The preliminarily reduced or oxidized (see Catalysts preparation section) Pt, Pd, Rh and Ir catalysts supported on titania were used for the heterogeneous hydrogenation of unsaturated hydrocarbons. The catalyst (30 mg) was placed at the bottom of a 10 mm NMR tube located inside an NMR spectrometer and maintained at 100 °C. The gas mixtures were supplied to the catalyst through a 1/16" OD PTFE capillary. Hydrogenation was performed in a 7.05 T magnetic field of the NMR spectrometer (the so-called PASADENA [13] experiment) at atmospheric pressure. The gas flow rate was varied from 1.4 to 5.7 mL/s using an Aalborg rotameter.

^{1}H NMR spectra of reaction mixtures in the gas phase were acquired with 8 signal accumulations on a 300 MHz Bruker AV 300 NMR spectrometer. A single π/4 radiofrequency pulse maximizing the PASADENA signal [16] was used to obtain the NMR spectra.

2.5. Calculation of conversion values and percentages of pairwise hydrogen addition

In the case of propene hydrogenation, two series of experiments (with p-H_2 and with normal H_2) were carried out successively with the same catalysts. It is known that the fast inflow of a fluid into an NMR instrument results in a substantial loss of an NMR signal for nominally thermally polarized molecules because of the insufficient residence time of the molecules in the high magnetic field to achieve a complete relaxation of nuclear spins to the high magnetic field equilibrium [26,37]. In the case of 1,3-butadiene hydrogenation, this problem can be solved by the use of the charcoal insert placed in the upper part of the NMR tube in the flow path of the incoming gas, which provides complete relaxation of 1,3-butadiene, 1-butene, 2-butene and butane nuclear spins to the equilibrium state at the 7.05 T field [26]. However, for propene hydrogenation this charcoal insert is unable to provide a complete recovery of propene and propane NMR signals [37]. Thereby, we used the approximations obtained in the previous study [37] by varying the flow rate of propene/H_2 and propane/H_2 gas mixtures in order to estimate the correct intensities of NMR signals. The propene conversion values X were calculated from these estimates of the fully recovered NMR signal intensities.

The percentages of pairwise H_2 addition were calculated as follows. The thermally polarized NMR spectra were subtracted from the corresponding spectra acquired with the use of parahydrogen. Therefore, the "pure" PASADENA spectra were obtained. The theoretical PASADENA signal enhancement factors (SEF) η can be calculated as [37]

$$\eta = \frac{4x_p - 1}{3}\frac{kT}{\gamma\hbar B_0} + 1 = 16500$$

where x_p is parahydrogen fraction in H_2 (0.83 in our experiments). However, in the case of PASADENA experiments the obtained polarization is reduced because of the partial cancellation of absorption and emission parts of each NMR signal and is thus dependent on the NMR line width. This fact was accounted for by comparing the simulated thermal and PHIP NMR spectra with the corresponding line width values, which allowed us to obtain the corrected theoretical SEF values κ depending on the NMR line width. The percentages of pairwise hydrogen addition $\phi_{pairwise}$ were calculated as

$$\phi_{pairwise} = \frac{\frac{S_{pol}}{\kappa}}{\frac{S_{pol}}{\kappa} + \frac{S_{therm}}{\mathrm{n}}}$$

where S_{pol} is the intensity of the absorption part of the "pure" PASADENA NMR signal, S_{therm} is the intensity of thermally polarized

Please cite this article in press as: O.G. Salnikov, et al., The effect of oxidative and reductive treatments of titania-supported metal catalysts on the pairwise hydrogen addition to unsaturated hydrocarbons, Catal. Today (2016), http://dx.doi.org/10.1016/j.cattod.2016.02.030

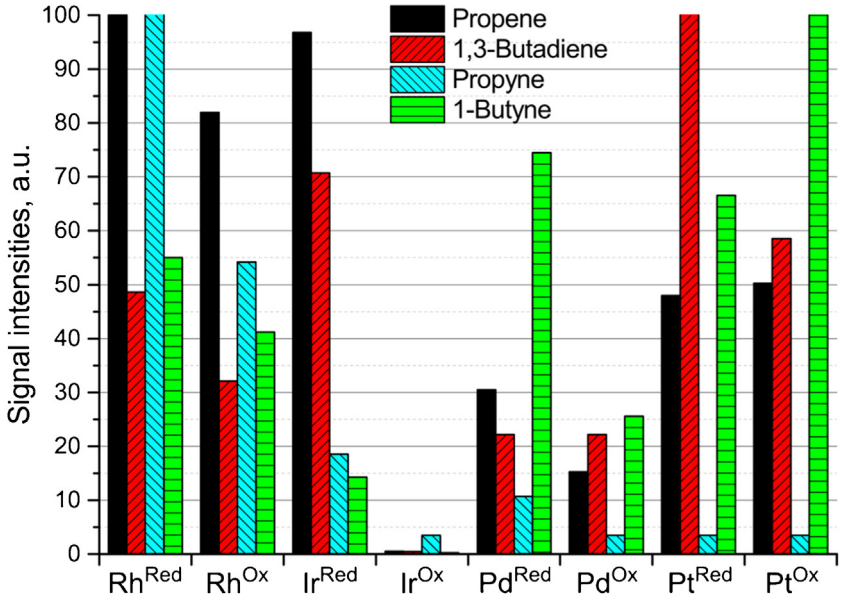

Fig. 2. The histogram of ^{1}H NMR signals intensities for various M^{Red}/TiO_2 and M^{Ox}/TiO_2 catalysts (see the figure legend for substrates designation). NMR signals were measured for CH_2-protons of propane in propene hydrogenation, CH_2-protons of butane in 1,3-butadiene hydrogenation, CH-proton of propene in propyne hydrogenation and CH-proton of 1-butene in 1-butyne hydrogenation. Note that the maximum achieved signal intensity for each substrate was set to 100 a.u., implying that NMR signal intensities can be compared only in the case of the *same* substrates. The gas flow rate was 4.1 mL/s in all of these experiments.

Table 1
The mean particle diameters for various M^{Red}/TiO_2 and M^{Ox}/TiO_2 catalysts calculated from HRTEM data.

Catalyst	Pt^{Red}/TiO_2	Pt^{Ox}/TiO_2	Pd^{Red}/TiO_2	Pd^{Ox}/TiO_2	Rh^{Red}/TiO_2	Rh^{Ox}/TiO_2	Ir^{Red}/TiO_2	Ir^{Ox}/TiO_2
Mean particle diameter (nm)	1.7	1.8	5.0	3.4[a]	1	0.6	1	0.7

[a] The particle size distribution is bimodal (ca. 1 nm and ca. 5 nm nanoparticles are observed).

NMR signal (corrected for suppression effects caused by the rapid gas inflow), and n is the number of corresponding protons ($n = 2$ for propane CH_2 group and $n = 6$ for propane CH_3 group). It should be noted that these percentages of pairwise hydrogen addition are largely underestimated because the relaxation of hyperpolarization as well as hydrogen ortho-para conversion were not taken into account. However, these two factors should not be significantly different for different catalysts due to the use of the same experimental conditions and a low concentration of supported metal; therefore, the estimated values of $\phi_{pairwise}$ can be compared with each other.

3. Results and discussion

Previously it was shown that titania-supported catalysts provide significantly more pronounced PHIP signals than alumina-, silica-, zirconia- or carbon-supported catalysts [26]. Therefore, in this study we utilized TiO_2-supported catalysts. The 5 wt% Pt/TiO_2, Pd/TiO_2, Rh/TiO_2 and Ir/TiO_2 catalysts were preliminarily reduced or oxidized (8 samples in total) and then used in hydrogenation of four hydrocarbons (propene, propyne, 1,3-butadiene and 1-butyne) with parahydrogen. The catalysts were characterized by both XPS and HRTEM before the hydrogenation reaction and by XPS after the reaction.

All catalysts except Ir^{Ox}/TiO_2 were found to be active in propene hydrogenation and most of them (except Ir^{Ox}/TiO_2 and Pd^{Ox}/TiO_2) produced pronounced PHIP NMR signals for propane when parahydrogen was utilized (Fig. 1). Moreover, ^{1}H NMR signals of propene (the reactant) were also polarized. This phenomenon, sometimes referred to as pairwise replacement, was previously observed for propene hydrogenation over 1 wt% Rh/TiO_2 [38], Pt/TiO_2 and Ir/TiO_2 [28] catalysts as well as over CeO_2 [30]. In this study, we found that pairwise replacement can be also provided by Rh^{Ox}/TiO_2 and Pt^{Ox}/TiO_2 as well as by Pd^{Red}/TiO_2 (Figs. 1 and S1).

It should be noted that in the previous heterogeneous PHIP investigations mostly 1 wt% supported metal catalysts were used [26,28]. Recently it was shown that in the case of catalytic systems with 1 wt% metal loading, the Rh/TiO_2 catalyst is more efficient in terms of production of hyperpolarized propane gas than Pt/TiO_2 and Pd/TiO_2 catalysts [23]. In another investigation, 1 wt% Pt/TiO_2 was found to be more efficient than Ir/TiO_2 [28]. However, herein we found that for 5 wt% catalysts Ir^{Red}/TiO_2 allows one to achieve PHIP NMR signals with nearly the same intensities as the corresponding Rh^{Red}/TiO_2 catalyst (Fig. 1d and c). This observation, without doubt, is very important and the 5 wt% Ir^{Red}/TiO_2 catalyst may represent a promising alternative for Rh/TiO_2 [23] for the production of hyperpolarized propane gas with the high level of polarization. Thus, in order to find an optimal catalyst for production of hyperpolarized propane gas it is highly important to vary a many parameters of the catalytic system such as the nature of the metal and the support, the size of metal nanoparticles and the metal content.

The percentages of pairwise H_2 addition for propene hydrogenation over these catalysts were estimated using both propane CH_2 and CH_3 groups NMR signals (Table S1). Note that the obtained values are slightly different because of the different relaxation properties of CH_2 and CH_3 protons of propane molecule. It can be seen that Pt^{Red}/TiO_2 and Pt^{Ox}/TiO_2 catalysts showed similar catalytic performance both in terms of PHIP and the overall conversion of propene to propane. On the other hand, Pd^{Red}/TiO_2 and Pd^{Ox}/TiO_2 were found to be similar in conversion but very different in terms of pairwise hydrogen addition. For Rh catalysts, the Rh^{Red}/TiO_2 provided a ca. 3 times higher contribution of pairwise hydrogen addition than Rh^{Ox}/TiO_2, while the latter provided signif-

Please cite this article in press as: O.G. Salnikov, et al., The effect of oxidative and reductive treatments of titania-supported metal catalysts on the pairwise hydrogen addition to unsaturated hydrocarbons, Catal. Today (2016), http://dx.doi.org/10.1016/j.cattod.2016.02.030

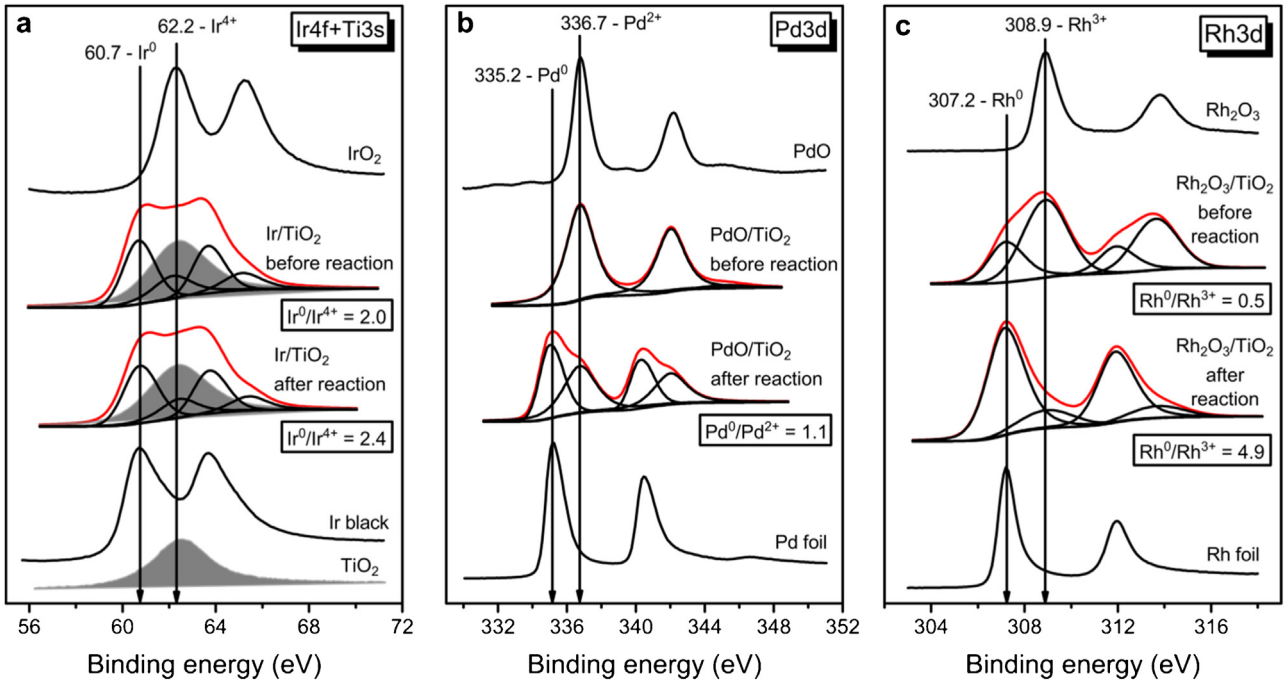

Fig. 3. (a) Ir 4f core-level XPS spectra of IrO_2/TiO_2 catalysts before and after propene hydrogenation reaction, Ir black and IrO_2 were used as references; (b) Pd 3d core-level XPS spectra of PdO/TiO_2 catalysts before and after propene hydrogenation reaction, Pd foil and PdO were used as references; (c) Rh 3d core-level XPS spectra of Rh_2O_3/TiO_2 catalysts before and after propene hydrogenation reaction, Rh foil and Rh_2O_3 were used as references. Binding energies are correlated to data from the XPS handbook [40].

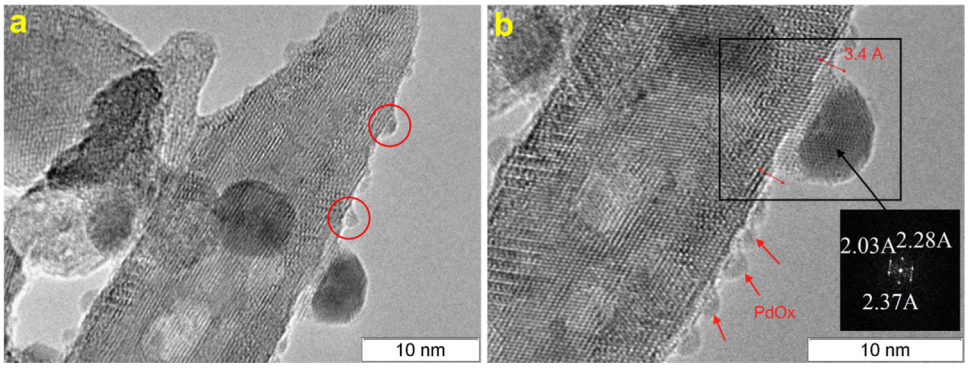

Fig. 4. HRTEM images of the Pd^{Ox}/TiO_2 sample. In (a) small ca. 1 nm nanoparticles are marked with circles. In (b) 3.4 Å thick titania pedestal with a large PdO particle on top of it is enclosed in a rectangle. The interplanar distances in PdO particles are presented in the black square. The arrows show small ca. 1 nm PdO_x particles.

icantly higher conversion. For Ir catalysts, the Ir^{Ox}/TiO_2 was found to be completely inactive in propene hydrogenation. Thereby, it may be concluded that in the case of heterogeneous hydrogenation of propene to propane over titania-supported Pd, Rh and Ir nanoparticles the oxidative treatment leads to a decrease in contribution of the pairwise hydrogen addition route (even down to zero in the case of palladium catalysts). On the contrary, maximum polarization and therefore the selectivity toward pairwise hydrogen addition are realized for a fully reduced M° state. These observations are in agreement with our recent SMSI investigations where formation of $Pd^{\delta+}$ sites for Pd/TiO_2 was found to completely destroy the pairwise hydrogen addition reaction pathway [34].

In the case of propyne, 1,3-butadiene and 1-butyne hydrogenation the PHIP results were generally similar (Figs. S2–S4). As in the case of propene hydrogenation, most of the catalysts provided PHIP NMR signals for corresponding reaction products. Ir^{Ox}/TiO_2 catalyst showed some negligible activity only in propyne hydrogenation where weak PHIP NMR signals were observed for reaction product propene (Figs. 2 and S2). In the case of 1,3-butadiene and 1-butyne hydrogenations, no reaction products were observed for the Ir^{Ox}/TiO_2 catalyst. Therefore, we can conclude that under our conditions Ir^{Ox}/TiO_2 is practically inactive in the hydrogenation reaction.

As was mentioned above, Pd^{Ox}/TiO_2 catalyst gave no PHIP effects in propene hydrogenation despite the observation of reaction products. The same was true in propyne hydrogenation (Fig. S2). However, in the case of 1,3-butadiene and 1-butyne hydrogenation over the Pd^{Ox}/TiO_2 catalyst, the PHIP effects were observed for various reaction products though their intensities were found to be not so high compared to the results obtained with other catalysts (Figs. S3 and S4). Therefore, the nature of the substrate is also important and may affect the pairwise hydrogen addition selectivity. In the case of propene and 1,3-butadiene hydrogenation over the Rh^{Red}/TiO_2 and Rh^{Ox}/TiO_2 catalysts, the formation of methane was observed (Figs. 1c and S3). However, there was no methane in propyne and 1-butyne hydrogenation in spite of the formation of mostly the same reaction products (Figs. S2 and S4), contrary to some literature data [39]. These results again show the importance of the substrate nature for the catalytic performance and the realization of different reaction pathways.

Please cite this article in press as: O.G. Salnikov, et al., The effect of oxidative and reductive treatments of titania-supported metal catalysts on the pairwise hydrogen addition to unsaturated hydrocarbons, Catal. Today (2016), http://dx.doi.org/10.1016/j.cattod.2016.02.030

With the aim to verify the structure of active sites, the catalysts were characterized using XPS and HRTEM methods. X-ray photoelectron spectra were acquired ex situ before and after hydrogenation reactions. In most of the preliminarily reduced catalysts (Pt^{Red}/TiO_2, Pd^{Red}/TiO_2 and Rh^{Red}/TiO_2) the corresponding metals were found to be in predominantly metallic states (Pt°, Pd° and Rh°, respectively). However, in the case of the Ir^{Red}/TiO_2 catalyst the starting material was found to contain both Ir° and Ir^{4+} in a 2:1 ratio (Fig. 3a). Upon propene hydrogenation the Ir° content increased only slightly (the Ir°/Ir^{4+} ratio became 2.4:1).

In the case of preliminarily oxidized catalysts the diverse results were obtained for each system. For the Pd^{Ox}/TiO_2 catalyst the corresponding metal was found to be in a pure oxide Pd^{2+} state (Fig. 3b). However, the XPS spectrum of the same Pd^{Ox}/TiO_2 catalyst after propene hydrogenation clearly exhibited a Pd° peak with corresponding 335.2 eV binding energy [40]. The Pd°/Pd^{2+} ratio in this material was found to be 1.1:1. Therefore, though the Pd^{Ox}/TiO_2 catalyst originally contained pure Pd^{2+}, it is partially reduced to Pd° in the course of the reaction. Similar results were obtained for the Pt/TiO_2 supported catalysts. However, for the Rh^{Ox}/TiO_2 catalyst the slightly different situation was found (Fig. 3c). According to XPS, the starting material contained both Rh° and Rh^{3+} with the prevalence of the latter (the Rh°/Rh^{3+} ratio 0.5:1). However, it should be mentioned that during 2 h of XPS measurements the decrease in Rh^{3+} and increase in Rh° peaks intensities were observed, implying that Rh oxide is gradually reduced under X-ray irradiation. Thus, it could be suggested that despite the use of a fast (just a few scans) recording of Rh 3d region for the XPS spectrum presented in Fig. 3c, the metal still undergoes partial reduction. Therefore, it is quite likely that initially Rh was in the oxide state (Rh^{3+}). Utilization of the catalyst sample in propene hydrogenation again led to a partial reduction of Rh^{3+} to Rh° because the Rh°/Rh^{3+} ratio was found to increase up to 4.9:1. On the other hand, in the Ir^{Ox}/TiO_2 material the metal was found to be in a pure Ir^{4+} state, both before and after the hydrogenation reaction. This is surely anticipated because as was mentioned above, this catalyst showed no activity in propene hydrogenation. Therefore, it is expected that the Ir^{4+} state remains unchanged during the exposure to propene/H_2 mixture. Based on XPS data it is easy to verify that partial reduction of metal oxide to metallic state occurs during hydrogenation reaction but this reduction is not enough for the formation of pure metal. Therefore, as it was mentioned above, the presence of oxidized state decreases the selectivity toward the pairwise hydrogen addition route.

Next, the HRTEM investigations were performed. The mean particles sizes of all catalysts are presented in Table 1. It was found that for Ir/TiO_2 and Pt/TiO_2 samples the oxidation and reduction procedures did not lead to significant changes in particle size. On the other hand, HRTEM revealed that though in Pt^{Red}/TiO_2 all Pt was found to be in Pt° state, in Pt^{Ox}/TiO_2 the metal was found to be in both metallic and oxide forms, although reduction of Pt under the electronic beam during HRTEM measurements cannot be excluded. For Rh/TiO_2 catalysts the mean particles diameter was found to slightly decrease from 1 to ca. 0.6 nm upon oxidation, although for Rh^{Ox}/TiO_2 the exact estimation of particle size is somewhat complicated because of their non-spherical shape. Interestingly, the mean particle sizes for 5 wt% Rh^{Red}/TiO_2 and Ir^{Red}/TiO_2 catalysts, which were found to be more efficient for production of hyperpolarized propane than other samples used in this study, are quite similar to the previously reported 1 wt% Rh/TiO_2 catalyst (ca. 1–1.5 nm) [23]. Another interesting fact is that for the Rh^{Red}/TiO_2 sample part of the active component was found to be in the Rh^{3+} state according to interplanar distances. According to HRTEM the TiO_2 surface was partly disordered, probably because of the interaction between the active component and the support and/or reduction of the support surface. For the Pd/TiO_2 systems HRTEM allowed to obtain some unique results. For Pd^{Red}/TiO_2 the particles with 5 nm mean diameter were observed. On the other hand, changes in anatase lattice distances and observation of palladium peaks in EDX spectra from these areas can be seen, meaning the occurrence of Pd clusters on the surface or in the bulk of TiO_2. For Pd^{Ox}/TiO_2 sample a bimodal particle size distribution was obtained. Besides relatively large nanoparticles 5–7 nm in diameter, small particles with ca. 1 nm size were observed on the anatase surface (Fig. 4a). According to interplanar distances these particles cannot be attributed to pure PdO or Pd, probably because of the partial reduction under electron beam to a $Pd^{\delta+}$ state (Fig. 4b). Another interesting fact is the formation of something like a pedestal from TiO_2 under larger PdO particles (Fig. 4b). The interplanar distances, both in pedestals and these PdO nanoparticles, are slightly different from the standard values.

As was mentioned above, in the Pt^{Red}/TiO_2 and Pt^{Ox}/TiO_2 samples the metal was found to be in the pure Pt° and Pt^{2+} states, respectively. However, the metal dispersion and the catalytic performance (including the selectivity toward pairwise hydrogen addition) of these catalysts were similar. Therefore, in the case of Pt the metal oxidation state has no significant impact on the catalytic performance, although the Pt^{Ox}/TiO_2 catalyst is partially reduced under hydrogenation conditions. For Rh catalysts the results are quite similar with those for Pt, although Rh^{Red}/TiO_2 was found to be slightly more efficient in terms of pairwise hydrogen addition than Rh^{Ox}/TiO_2. This can be explained by the fact that Rh^{3+} is significantly reduced to Rh° during the reaction (according to XPS data, the Rh^{3+} fraction decreased from 67% to 17%). Therefore, it can be concluded that on the Rh° the contribution of pairwise hydrogen addition route is higher than on Rh^{3+}. On the other hand, the catalytic performances of Ir^{Red}/TiO_2 and Ir^{Ox}/TiO_2 catalysts in heterogeneous hydrogenations were found to be dramatically different despite the fact that no significant alterations in metal nanoparticles size were observed. Therefore, these differences in activities correlate with Ir oxidation state. In Ir^{Ox}/TiO_2 sample all metal is in the Ir^{4+} state. On the other hand, in catalytically active Ir^{Red}/TiO_2 sample both Ir° and Ir^{4+} states were observed. Therefore, it is possible that only Ir° but not Ir^{4+} can catalyze hydrogenation of hydrocarbons as well as be responsible for pairwise hydrogen addition. As for the properties of Pd^{Red}/TiO_2 and Pd^{Ox}/TiO_2 samples, they were found to be strongly different. First of all, the metal in these two samples was initially in different oxidation states (Pd° and Pd^{2+}, respectively), although partial reduction of Pd^{2+} to Pd° during hydrogenation was detected. Moreover, while in the case of Pd^{Red}/TiO_2 the particles size was ca. 5.0 nm, the Pd^{Ox}/TiO_2 catalyst contained both large (ca. 5–7 nm) and small (ca. 1 nm) particles located predominantly at the facets of TiO_2 support. Also for the first time the HRTEM revealed the formation of TiO_2 pedestals under Pd particles. As for the catalytic performance, the Pd^{Ox}/TiO_2 catalyst exhibited significantly lower efficiency in terms of pairwise hydrogen addition (no PHIP effects in propene and propyne hydrogenation and less intensive PHIP effects in 1,3-butadiene and 1-butyne hydrogenation). Our hypothesis is that the reason for this is the formation of $Pd^{\delta+}$ sites which are fully inconsistent with pairwise hydrogen addition. Without doubt, the change in interplanar distances, the formation of Pd clusters, the modification of electronic structure of PdO particles via pedestals formation allow to block Pd° sites which are required for the pairwise hydrogen addition.

4. Conclusions

In this study, titania-supported Pt, Pd, Rh and Ir catalysts were utilized for hydrogenation of unsaturated hydrocarbons (propene, propyne, 1,3-butadiene and 1-butyne) with parahydrogen. It was shown that the oxidation or reduction of the catalysts impact significantly on the overall catalytic activity and, more importantly, on

Please cite this article in press as: O.G. Salnikov, et al., The effect of oxidative and reductive treatments of titania-supported metal catalysts on the pairwise hydrogen addition to unsaturated hydrocarbons, Catal. Today (2016), http://dx.doi.org/10.1016/j.cattod.2016.02.030

the selectivity toward pairwise hydrogen addition to a substrate, i.e., the ability to incorporate both H atoms of an H_2 molecule into the same product molecule. Generally, for M° the contribution of pairwise hydrogen addition route was found to be higher than for M^{n+} in the case of titania-supported catalytic systems. For instance, formation of $Pd^{\delta+}$ sites or insufficient reduction of Pd^{2+} to Pd° leads to a decrease in the PHIP signals intensities and therefore, to a lower contribution of pairwise hydrogen addition. The formation of titania pedestals with PdO particles on their top was observed by HRTEM for the first time for Pd/TiO_2 catalyst. The 5 wt% Ir°/TiO_2 catalyst was found to demonstrate nearly the same efficiency for production of hyperpolarized propane as the corresponding Rh/TiO_2 catalyst. Thereby, it is a good alternative to Rh/TiO_2, which was earlier shown to be the most efficient for producing PHIP effects in this reaction. Although the pairwise hydrogen addition route contributes only a few percent to the overall hydrogenation reaction mechanism, the improvement of the catalysts preparation procedure and the identification of the structure of active sites responsible for pairwise hydrogen addition can in perspective further improve the selectivity toward pairwise route and therefore, significantly enhance NMR and MRI sensitivity.

Acknowledgments

OGS, DBB, DAB, KVK, and IVK thank RSCF (grant #14-13-00445) for supporting the catalytic hydrogenation experiments using parahydrogen and the high-field NMR studies. IPP and EYG thank RFBR (grants ## 14-03-00374-а and 14-03-93183 МСХ_а) for the support of XPS and HRTEM studies. VIB, AKK, LMK and AVB thank RSCF (grant #14-23-00146) for supporting the catalysts preparation. The basic funding of the SB RAS institutes was provided by FASO.

Appendix A. Supplementary data

Supplementary data associated with this article can be found, in the online version, at http://dx.doi.org/10.1016/j.cattod.2016.02.030.

References

[1] B.M. Weckhuysen, Angew. Chem. Int. Ed. 48 (2009) 4910–4943.
[2] S. Mitchell, N.-L. Michels, G. Majano, J. Pérez-Ramírez, Curr. Opin. Chem. Eng. 2 (2013) 304–311.
[3] J.C.J. Camp, M.D. Mantle, A.P.E. York, J. McGregor, Rev. Sci. Instrum. 85 (2014) 063111.
[4] T. Titze, C. Chmelik, J. Kullmann, L. Prager, E. Miersemann, R. Gläser, D. Enke, J. Weitkamp, J. Kärger, Angew. Chem. Int. Ed. 54 (2015) 5060–5064.
[5] C. Sievers, S.R. Bare, E. Stavitski, The 4th international congress on operando spectroscopy, Catal. Today 205 (2013).
[6] I.V. Koptyug, Magnetic resonance imaging methods in heterogeneous catalysis, in: R. Douthwaite, S. Duckett, J. Yarwood (Eds.), Spectrosc. Prop. Inorg. Organomet. Compd., Royal Society of Chemistry, Cambridge, 2014, pp. 1–42.
[7] A.A. Lysova, I.V. Koptyug, Chem. Soc. Rev. 39 (2010) 4585–4601.
[8] L.F. Gladden, Curr. Opin. Chem. Eng. 2 (2013) 331–337.
[9] P. Nikolaou, B.M. Goodson, E.Y. Chekmenev, Chem. Eur. J. 21 (2015) 3156–3166.
[10] J.-H. Ardenkjaer-Larsen, G.S. Boebinger, A. Comment, S. Duckett, A.S. Edison, F. Engelke, C. Griesinger, R.G. Griffin, C. Hilty, H. Maeda, G. Parigi, T. Prisner, E. Ravera, J. van Bentum, S. Vega, A. Webb, C. Luchinat, H. Schwalbe, L. Frydman, Angew. Chem. Int. Ed. 54 (2015) 9162–9185.
[11] R.G. Griffin, T.F. Prisner, Phys. Chem. Chem. Phys. 12 (2010) 5737–5740.
[12] B.M. Goodson, J. Magn. Reson. 155 (2002) 157–216.
[13] C.R. Bowers, D.P. Weitekamp, J. Am. Chem. Soc. 109 (1987) 5541–5542.
[14] R.A. Green, R.W. Adams, S.B. Duckett, R.E. Mewis, D.C. Williamson, G.G.R. Green, Prog. Nucl. Magn. Reson. Spectrosc. 67 (2012) 1–48.
[15] C.R. Bowers, D.P. Weitekamp, Phys. Rev. Lett. 57 (1986) 2645–2648.
[16] C.R. Bowers, Sensitivity enhancement utilizing parahydrogen, in: D.M. Grant, R.K. Harris (Eds.), Encycl. Magn. Reson., John Wiley & Sons, Ltd., Chichester, 2002, pp. 750–770.
[17] D. Blazina, S.B. Duckett, J.P. Dunne, C. Godard, Dalton Trans. (2004) 2601–2609.
[18] T.C. Eisenschmid, R.U. Kirss, P.P. Deutsch, S.I. Hommeltoft, R. Eisenberg, J. Bargon, R.G. Lawler, A.L. Balch, J. Am. Chem. Soc. 109 (1987) 8089–8091.
[19] L. Buljubasich, M.B. Franzoni, K. Munnemann, Parahydrogen induced polarization by homogeneous catalysis: theory and applications, in: L.T. Kuhn (Ed.), Hyperpolarization Methods NMR Spectrosc, Springer-Verlag, Berlin, 2013, pp. 33–74.
[20] S. Glöggler, J. Colell, S. Appelt, J. Magn. Reson. 235 (2013) 130–142.
[21] I. Horiuti, M. Polanyi, Trans. Faraday Soc. 30 (1934) 1164–1172.
[22] K.V. Kovtunov, I.E. Beck, V.I. Bukhtiyarov, I.V. Koptyug, Angew. Chem. Int. Ed. 47 (2008) 1492–1495.
[23] K.V. Kovtunov, D.A. Barskiy, A.M. Coffey, M.L. Truong, O.G. Salnikov, A.K. Khudorozhkov, E.A. Inozemtseva, I.P. Prosvirin, V.I. Bukhtiyarov, K.W. Waddell, E.Y. Chekmenev, I.V. Koptyug, Chem.—A Eur. J. 20 (2014) 11636–11639.
[24] S.S. Arzumanov, A.G. Stepanov, J. Phys. Chem. C. 117 (2013) 2888–2892.
[25] R. Zhou, W. Cheng, L.M. Neal, E.W. Zhao, K. Ludden, H.E. Hagelin-Weaver, C.R. Bowers, Phys. Chem. Chem. Phys. 17 (2015) 26121–26129.
[26] K.V. Kovtunov, V.V. Zhivonitko, I.V. Skovpin, D.A. Barskiy, I.V. Koptyug, Parahydrogen-Induced polarization in heterogeneous catalytic processes, in: L.T. Kuhn (Ed.), Hyperpolarization Methods NMR Spectrosc., Springer-Verlag, Berlin, 2013, pp. 123–180.
[27] O.G. Salnikov, K.V. Kovtunov, D.A. Barskiy, A.K. Khudorozhkov, E.A. Inozemtseva, I.P. Prosvirin, V.I. Bukhtiyarov, I.V. Koptyug, ACS Catal. 4 (2014) 2022–2028.
[28] R. Zhou, E.W. Zhao, W. Cheng, L.M. Neal, H. Zheng, R.E. Quiñones, H.E. Hagelin-Weaver, C.R. Bowers, J. Am. Chem. Soc. 137 (2015) 1938–1946.
[29] K.V. Kovtunov, D.A. Barskiy, O.G. Salnikov, A.K. Khudorozhkov, V.I. Bukhtiyarov, I.P. Prosvirin, I.V. Koptyug, Chem. Commun. 50 (2014) 875–878.
[30] E.W. Zhao, H. Zheng, R. Zhou, H.E. Hagelin-Weaver, C.R. Bowers, Angew. Chem. Int. Ed. 54 (2015) 14270–14275.
[31] A.M. Balu, S.B. Duckett, R. Luque, Dalton Trans. (2009) 5074–5076.
[32] O.G. Salnikov, K.V. Kovtunov, I.V. Koptyug, Sci. Rep. 5 (2015) 13930.
[33] S. Gloggler, A.M. Grunfeld, Y.N. Ertas, J. McCormick, S. Wagner, P.P.M. Schleker, L.-S. Bouchard, Angew. Chem. Int. Ed. 54 (2015) 2452–2456.
[34] K.V. Kovtunov, D.A. Barskiy, O.G. Salnikov, D.B. Burueva, A.K. Khudorozhkov, A.V. Bukhtiyarov, I.P. Prosvirin, E.Y. Gerasimov, V.I. Bukhtiyarov, I.V. Koptyug, ChemCatChem 7 (2015) 2581–2584.
[35] K.V. Kovtunov, M.L. Truong, D.A. Barskiy, I.V. Koptyug, A.M. Coffey, K.W. Waddell, E.Y. Chekmenev, Chem. —A Eur. J. 20 (2014) 14629–14632.
[36] http://xpspeak.software.informer.com/4.1/.
[37] D.A. Barskiy, O.G. Salnikov, K.V. Kovtunov, I.V. Koptyug, J. Phys. Chem. A 119 (2015) 996–1006.
[38] K.V. Kovtunov, M.L. Truong, D.A. Barskiy, O.G. Salnikov, V.I. Bukhtiyarov, A.M. Coffey, K.W. Waddell, I.V. Koptyug, E.Y. Chekmenev, J. Phys. Chem. C 118 (2014) 28234–28243.
[39] B.J. Brandreth, S.D. Jackson, D. Winstanley, J. Catal. 102 (1986) 433–442.
[40] J.F. Moulder, W.F. Stickle, P.E. Sobol, K. Bomben, Handbook of X-ray Photoelectron Spectroscopy, 2nd ed., Perkin-Elmer Corporation, Eden Priarie, MN, 1992.

Please cite this article in press as: O.G. Salnikov, et al., The effect of oxidative and reductive treatments of titania-supported metal catalysts on the pairwise hydrogen addition to unsaturated hydrocarbons, Catal. Today (2016), http://dx.doi.org/10.1016/j.cattod.2016.02.030